An FL-PID Mixed Technique to Control a Military Rocket Launcher System Board

Jeki Saputra[1] and Rini Nur Hasanah[2]
[1]*Department of Weapon System Electronics, Polytechnics of Indonesian Army (Poltekad), Indonesia*
[2]*Department of Electrical Engineering, Faculty of Engineering, Brawijaya University, Indonesia*.
jeki8422@yahoo.co.id

***Abstract*—This article proposes the design and construction of an automatic launcher system for military weaponry. Combining the fuzzy-logic and proportional-integral-differential control theories, the launcher system board is purposed to automatically direct a military rocket along its azimuth and elevation angles direction. The fuzzy-logic method has been explored to find the values of K_p, K_i and K_d constants of a proportional-integral-differential controller, which will then be used to adjust the angular position of actuator according to a predetermined set-point. The combined control algorithm has been implanted on the Arduino Mega 2560 and implemented to launch the 70 mm-caliber *Rolex* rocket being considered during the experiment. Successful control result, which was indicated with the average steady-state error value of 0%, has been resulted.**

***Index Terms*—Fuzzy-Logic Control; Military Weaponry; PID Control; Rocket Launcher.**

I. INTRODUCTION

The military defense autonomy in a country is of paramount importance to protect from any internal and external threats to its security and to ensure its sovereignty [1]. Upgrading and improvement of weaponry in a military system should be able to keep up with the technology advancement. The physical defense equipment can be generally divided into three categories, associated with the land, sea, and air defense fields, besides the defense in terms of cyber security, strategies, etc. [2],[3]. One of the important artillery in the military world is a rocket.

A rocket is a missile, spacecraft, aircraft or another vehicle which obtains its thrusting force from the results of propellant combustion in a rocket engine. The engines push rockets forward simply by expelling their exhaust in the opposite direction at a high speed [4],[5]. The components of a rocket include a warhead, body, propellant, fins, and nozzle, and the other related supporting equipments. The warhead is used to destroy the targets in the event of collision, the body serves to protect the rocket components, the propellant is a source of energy through the combustion reaction, the fins are used to maintain the stability of the rocket movement, whereas the nozzle serves to distribute, to boost and to accelerate the flow of hot exhaust gas being resulted from the propellant combustion [6].

As a part of its training and education program, the Center for Education and Training of the Indonesian Army through its Technology Research Institute has created an experiment rocket for the training purpose, being called the 70 mm-caliber *Rolex* trainer rocket. With the length of 1400 mm, it uses a propellant of ammonium perchlorate (AP), aluminum (Al), and hydroxyl-terminated polybutadiene (HTPB). The rocket has been proven feasible during the test, but it is still using a manual control system to establish the launcher's motion stability [1]-[3].

The rocket launcher movement is directed by raising or lowering the elevation angle and then tightening the locking hook of the launcher. The *Rolex* trainer rocket will be ready for firing the target once the right elevation angle is achieved. The process of determining the angle of the rocket launcher movement requires quite a long time because the power needed to drive the rocket launcher is quite large, considering its material substance which is containing iron steel and aluminum.

In this article, it is proposed to help the rocket operator to automatically drive and direct the *Rolex* rocket launcher into the desired position. The azimuth and elevation angles are to be controlled by performing a mixed control technique based on the fuzzy logic (FL) theory and the proportional-integral-differential (PID) control theory. The FL theory is used to determine the value of K_p, K_i and K_d constants of the PID controller, which is then used to set the motor angle so that it can be maintained in accordance with the desired setpoint value. The position control algorithm is to be implanted on an Arduino Mega 2560 and to be implemented using a rocket launching board being driven by a DC motor [2]-[3],[7].

II. DESIGN AND CONTROL METHODS

A. The Rocket Launcher System to Build

The schematic diagram representing the working principle of the rocket launcher system to build is given in Figure 1. The keypad is used to give the instruction about the azimuth and elevation angles of the position to direct by the actuator. The information is then processed by the microcontroller and displayed by the LCD screen.

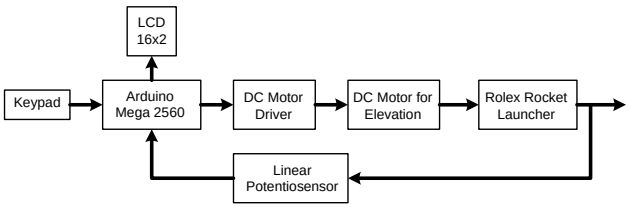

Figure 1: The Working Principle of The Rocket Launcher System

The Arduino Mega 2560 microcontroller processes the input data which are given through the keypad to instruct the motor to move. The driver controls the direction and the speed of the DC motor movement based on the instructions from the microcontroller. The linear potentiometer will

provide the voltage output which varies according to the position of the DC motor at the respective moment.

B. 70-mm Rolex Experiment Trainer Rocket

A rocket is a missile which produces thrusting forces coming from the combustion of asolid propellant. The propellant is composed of the mixture of Potassium Nitrate (KNO_3), which is classified as a low-explosive fuel, and Sorbitol. Sorbitol is a chemical substance which is odorless, water-resistant, and in the form of a clear liquid or a white powder crystalline. It is used as a binder agent and identified as a potential key chemical intermediate for production of fuels from biomass resources [6].

The main parts of a rocket include nose cone (1), tube (2), igniter (3), propellant (4), launch lug (5), fins (6), and nozzle (7), as shown in Figure 2. The specifications of the rocket body considered in this paper are given in Table 1 [4],[5].

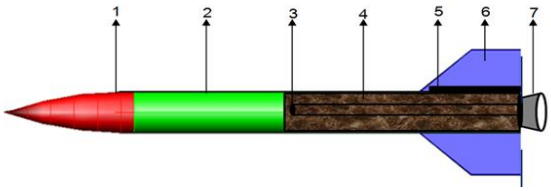

Figure 2: The Main Parts of The 70-mm Rolex Rocket

C. 70-mm Rocket Launcher

A rocket launcher is used to help to launch and direct the movement of a rocket. The main parts of a rocket launcher cover the directing launcher (1), nuts and bolts on the elevation shaft (2), azimuthal shaft and bearings (3), and tripod (4), as seen in Figure 3. The specifications concerning the related material, dimension and weight are given in Table 1.

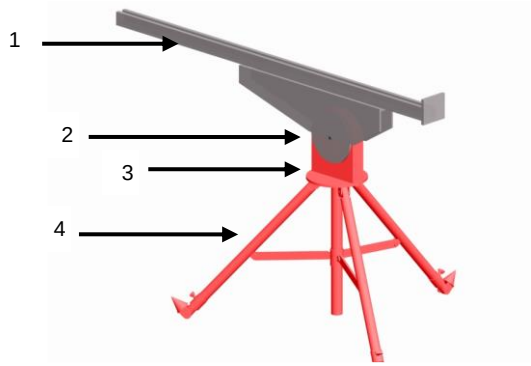

Figure 3: The Main Parts of The 70-mm *Rolex RX B-17/SADIS* Rocket Launcher

D. The Control Method

The design and construction of the rocket launcher system are based on the combination of the fuzzy logic (FL) theory and the proportional-integral-differential (PID) control theory [2-3],[7]. The combination technique is to be implemented by utilizing the Arduino Mega 2560 microcontroller technology. The design includes the hardware and software parts and is adapted to the specifications of the actual *Rolex* rocket. Sensors are used to detect the input data before being processed by the microcontroller.

The purpose is to control the movement of the rocket launcher automatically. The control system establishes an intelligent control which utilizes the error and delta error of the angular position of the rocket launcher as inputs. Based on the membership functions in the FL control system, the input data will be processed to produce the outputs to determine the values of K_p, K_i and K_d constants of the PID controller. By using DC motors as actuators, the control system will drive the rocket launcher to move in the direction of azimuth and elevation angles based on the setpoint data input given using a keypad.

Table 1
The Specification of the Rocket Body and Rocket Launcher

Component	Part name	Note
Rocket body	Body material	Aluminum
	Body length	120 cm
	Body diameter	70 mm
	Body thickness	2 mm
	Nose material	Nylon and iron
	Nose length	20 cm
	Nose empty weight	4.5 kg
	Nose total weight	7.85 kg
Rocket launcher	Body material	Aluminum
	Body length	120 cm
	Body diameter	70 mm
	Body thickness	2 mm
	Nose material	Nylon and iron
	Nose length	20 cm
	Nose empty weight	4.5 kg
	Nose total weight	7.85 kg

In a control system, it is desired to undertake and accomplish certain assigned task. It is required that a control system be stable. It must be able to perform the task with certain stability criteria, which comprise both the absolute and relative stabilities [8],[9]. The relative stability is a quality measure of stability by considering its condition if being exposed to disturbance. Stability analysis is also required to get the information on how fast the system responds to the incoming inputs and how fast any overshoot is damped.

Some control actions can be of proportional, integral, and derivative characteristics. Each action possesses its specific advantages. Proportional (P) control action offers short rise-time, integral (I) control action serves to reduce error, while derivative (D) control action can predict system behavior to improve the settling time and stability of the system. The tuning of the PID control parameters is a difficult problem [8]. When being used alone, the PID controllers may result in a poor performance, especially when the loop gains must be reduced to avoid any overshoot, oscillation or hunting around certain setpoint value.

The fuzzy-logic theory offers an alternative approach to conventional methods without relying on mathematical models [10-17]. It has been inspired by the way a human is thinking. It applies the human ability system to solve problems by assigning certain rules. The IF-THEN rules can be applied to process control action by using linguistic approach, forming a fuzzy-logic control. This kind of control does not depend on the control variables and has been developed in the control engineering field especially for nonlinear and dynamic systems. For many industrial control needs, this type of control offers alternative solutions to the tuning difficulty problems of the PID controllers. In this study, it is applied to set the PID controller parameters K_p, K_i and K_d to form a mixed FL-PID control method.

E. Fuzzification and De-fuzzification Processes

Fuzzification is the step to transform the crisp sets into fuzzy sets. The crisp sets are the input data commonly obtained from the measurements using sensors, for temperature, pressure, etc. The fuzzification process uses fuzzy linguistic variables, fuzzy linguistic terms and membership functions. Furthermore, based on a set of rules an inference is made [16],[17].

Input and output variables for error and Δerror are given in Equation (1) and (2).

$$Error(t) = SP - PV(t) \tag{1}$$

$$\Delta Error = Error(t) - Error(t-1) \tag{2}$$

where: *SP* = *Set Point* of the desired value
PV = *Present Value* representing the actual value at time *t*
Error(*t*) = *error* value at time *t*
Error(*t-1*) = *error* value at time (*t-1*)

The membership functions of the *error* and Δ*error* are shown in Figure 4 and Figure 5 respectively. The fuzzification rules to be applied are indicated in Figure 6, whereas the membership function of the output is given in Figure 7.

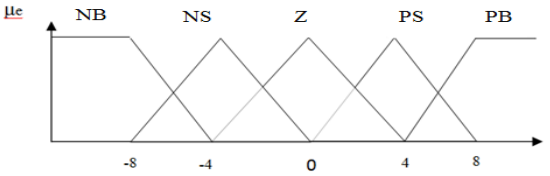

Figure 4: The Membership Function of *error*

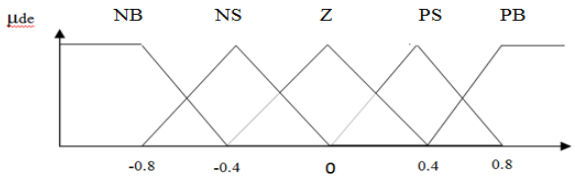

Figure 5: The Membership Function Of Δ*Error*

		e				
		NB	NS	Z	PS	PB
de	NB	PB	PB	PB	PS	PS
	NS	PB	PB	PS	NS	NS
	Z	PB	PS	NS	NS	NB
	PS	PS	PS	NS	NB	NB
	PB	PS	NS	NS	NB	NB

Figure 6: The Fuzzification Rules

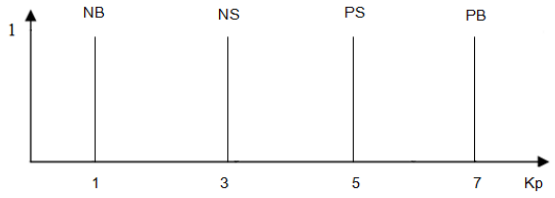

Figure 7: The Membership Function of The *Output*

The defuzzification process is needed in the fuzzy control systems to produce a quantifiable result in a form of crisp logic, being given certain fuzzy sets and its corresponding membership degrees. It is to set the values of K_p, K_i and K_d constants of the PID controllers. The adopted defuzzification method was the singleton one, as expressed by the following equation:

$$U = \frac{\sum_{i=1}^{n} w_i u_i}{\sum_{i=1}^{n} w_i} \tag{3}$$

where: U = output
w_i = the weight of true w_i
u_i = the linguistic value on the membership function of outputs
n = the membership degree number

F. Implementation into Microcontroller

To input the setpoint value, a keypad 4x4 and an LCD 16x2 have been used. The keypad contains a set of buttons arranged in a block bearing some digits, being used to give the desired numeric input. The LCD (Liquid Crystal Display) screen is an electronic display module which is very economical, easily programmable, have no limitation of displaying special and even custom characters (unlike in its seven segments counterparts), animations and so on with low current consumption. A 16x2 LCD displays 16 characters per line and there are 2 such lines. The dot matrix LCD module M1632 being made by Hitachi is considered in this paper. It consists of two parts; one is to display the characters, the other is the LCD processor system whose function is to set the LCD display as well as the communications between the LCD and the microcontroller [18]-[20].

The considered microcontroller during the research was the Arduino Mega 2560. It is a microcontroller board based on the high-performance, low-power Microchip 8-bit AVR RISC-based Atmega2560 microcontroller. Possessing 54 digital input/output pins, of which 15 can be used as PWM outputs, this board provides 16 analog inputs, 4 UARTs (hardware serial ports), a 16 MHz crystal oscillator, a USB connection, a power jack, an ICSP header, and a reset button.

The ATMega 2560 board can be programmed with the Arduino Software (IDE/Integrated Development Environment). This application software provides the possibility to write and to compile the Arduino program, to debug it whenever an error is produced, as well as to upload it to the Arduino board. The block diagrams of the motion control along the azimuthal and elevation angle directions are shown in Figs. 8 and 9 respectively.

G. Direct-Current Motor as Actuator

In this research article, the main actuator to effectuate the movement based on the command from the controller is a direct-current (DC) motor. It is an electric motor which requires direct-current voltage supply on its field winding to be converted into mechanical rotation. The field winding constitutes the stator, whereas the armature winding constitutes the rotor. The circuit schema and the driver for

the motor are shown in Figure 10 and Figure 11 respectively.

The actuator is used to drive a device to launch a rocket-propelled projectile. Its firing target direction is governed through the azimuthal and elevation angular positions. In the military application in general, the launcher is commonly mounted on a vehicle, such as trucks or tractor units to transport or launch missiles (rockets with warheads), as seen in Figure 12. Such a vehicle may transport one or multiple missiles. The missile vehicle may be a self-propelled unit or the missile holder/launcher may be on a trailer towed by a prime mover. They are used in the military forces of a number of countries in the world.

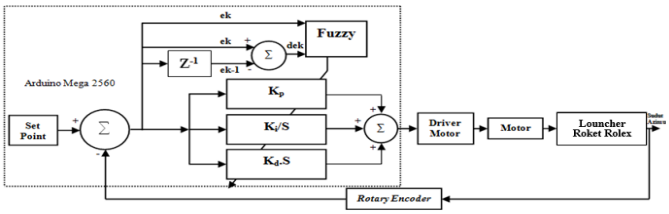

Figure 8: The Block Diagram of The System Movement Control Along The Azimuthal Direction

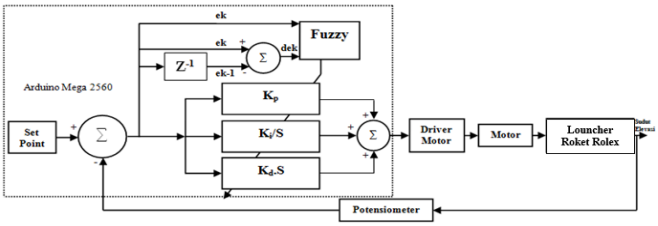

Figure 9: The Block Diagram of The System Movement Control Along The Elevation Angle Direction

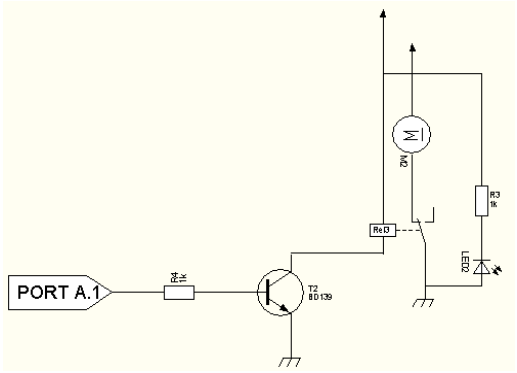

Figure 10: The Circuit Schema of The DC Motor System

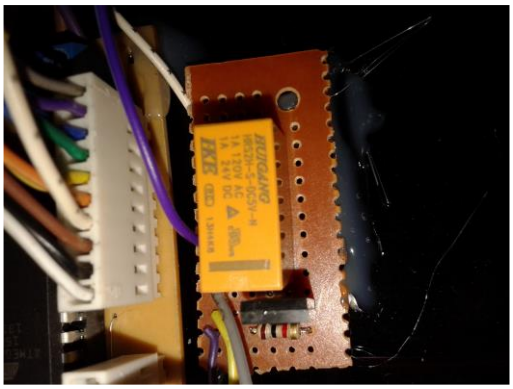

Figure 11: The Driver Circuit of The DC Motor

The design of the mechanical launcher system of this paper is shown in Figure 13, whereas the related construction is given in Figure 14. As can be seen, the keypad and LCD displays are used to input the setpoint values, whereas as the mounting support has been used a tripod.

Figure 12: A Typical Rocket Launcher Vehicle

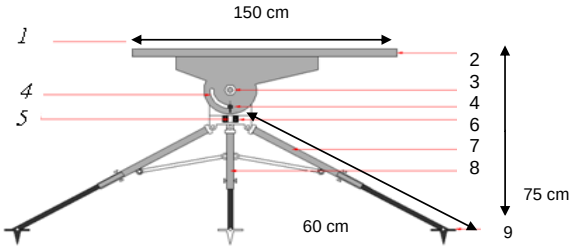

Figure 13: The Mechanical Launcher System Design

Figure 14: The Construction Of The Mechanical Launcher System

III. Results and Discussion

The experiments have been performed to verify whether the designed system would work as specified and desired. The experiment results needed to be analyzed by refereeing to the prevailing theory.

The system uses an Arduino Mega 2560, 2 DC-motors, 2 modules of EMS 30A H-bridge DC motor driver, 1 potentiometer, 1 rotary encoder, and 1 keypad. The Arduino serves as the data processor and the interface with keypad, DC motors, and to process the mixed control algorithm using FL and PID methods. The EMS 30A H-bridge motor driver module is an H-bridge driver designed to produce 2-way driving mechanism using DC current up to 30 A in the range of voltage of 5-36 Volts. The potentiometer is used to detect the magnitude of the elevation angles of the rocket launcher. The rotary encoder sensors are used to count the pulse-number interpreting the number of DC motor rotations related to azimuthal angles. The two DC motors serve to actuate the launcher in the elevation and azimuthal directions.

A. Testing Results of the Potentiometer

A linear potentiometer has been used to measure the angular position of the DC motor rotation. It was installed in parallel with the DC motor so that each change in the rotational angle of the motor will have a direct effect on the resistance change of the potentiometer. The design and construction of the linear potentiometer system considered in this paper are given in Figure 15.

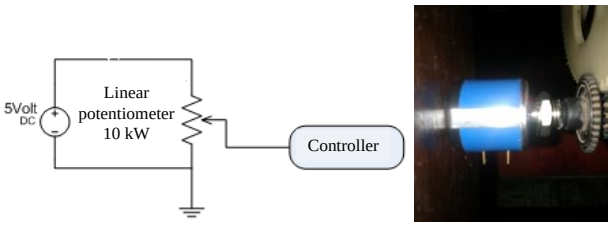

Figure 15: The Design and Construction of The Linear Potentiometer System

The output voltage of the potentiometer is obtained using Equation (4), whereas the measurement error is obtained using Equation (5).

$$V_{output} = \frac{R_{potentiometer}}{R_{total}} \text{ x } V_{input} \quad (4)$$

$$Error(\%) = \frac{V_{measured} - V_{calculated}}{V_{measured}} \text{ x } 100\% \quad (5)$$

where: V_{output} = output voltage of the potentiometer
$R_{potentiometer}$ = resistance of the potentiometer
R_{total} = total resistance of the circuit
V_{input} = input voltage of the potentiometer
$Error$ = the measurement error
$V_{measured}$ = the measured voltage
$V_{calculated}$ = the calculated voltage

The testing result data are given in Table 2, whereas the resistance and the voltage of the potentiometer as a function of rotation angle of the motor are given in Figure 16 and Figure 17 respectively.

Table 2, Figure 16 and Figure 17 indicate that the considered potentiometer worked well as desired. It is shown by the linear relationship between the motor rotation angle and the resulted resistance and voltage of the potentiometer, which is also confirmed by the average error between the calculated value and the measured value. Consequently, the potentiometer can be used in the designed system, to detect the angular position of the DC motor rotation in actuating the launcher until the certain angular position as determined using the setpoint value.

B. Testing Results of the Whole System Functioning

The overall system testing is done to find out whether the whole system components, both the hardware and the software parts, can work together in an integrated system. The whole system is shown in Figure 18.

As can be seen in Figure 18, there are two power supplies of 5V and 12V, the main plant which is the rocket launcher including 2 DC motors as actuator and rotary encoder, the potentiometer, the motor driver, and the keypad as well as the microcontroller which must be equipped with an appropriate program and its related programming language.

Table 2
The Results of Potentiometer Testing

Angle [^{O}]	Resistance [kΩ]	Measured voltage [V]	Calculated voltage [V]	Error [%]	Angle [^{O}]
0	1	0.498	0.50000	0.39900	0
15	1.25	0.626	0.62499	0.16100	15
30	1.5	0.754	0.74999	0.57874	30
45	1.75	0.883	0.87499	0.91529	45
60	2	0.999	0.99999	0.13230	60
75	2.25	1.145	1.12499	1.77880	75
90	2.5	1.267	1.24999	1.38765	90
105	2.75	1.391	1.37499	1.16465	105
120	3	1.502	1.49999	0.13433	120
135	3.25	1.651	1.62498	1.60102	135
150	3.5	1.782	1.74998	1.81056	150
165	3.75	1.967	1.87498	4.90772	165
180	4	2.002	1.99998	0.10100	180
195	4.25	2.189	2.12498	3.01279	195
210	4.5	2.304	2.24998	2.38622	210
225	4.75	2.436	2.37498	2.56945	225
240	5	2.524	2.49998	0.94769	240
255	5.25	2.712	2.62497	3.31532	255
270	5.5	2.757	2.74997	3.15256	270
285	5.75	2.837	2.87497	3.34016	285
300	5.75	2.971	2.99997	0.11010	300

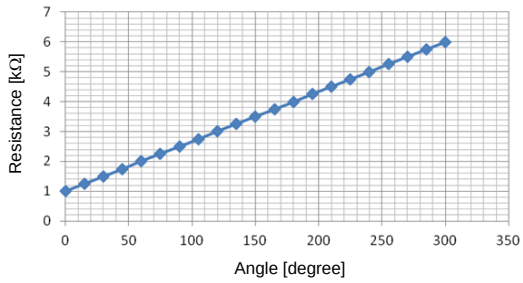

Figure 16: The Relationship Between The Motor Rotation Angle And The Resistance of The Potentiometer

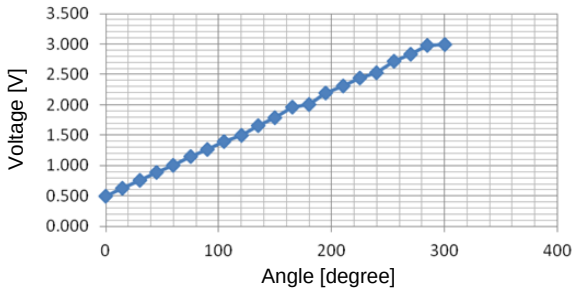

Figure 17: The Relationship Between The Motor Rotation Angle And The Voltage of The Potentiometer

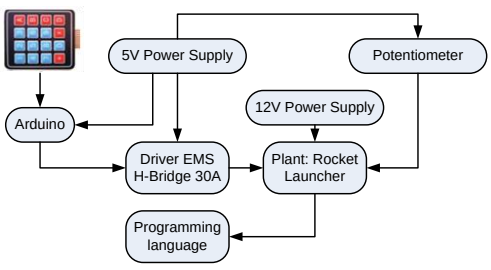

Figure 18: The experiment set-up for the whole system functioning

The algorithm of mixed FL-PID control technique has been implanted into the Arduino after being written into some executable instructions using the appropriate programming language. The required power has been provided using the 5V and 12V supplies, being adapted to the requirement of each component. The data of angular position, motor rotation, and also the setpoint input from the keypad, have been used to obtain the graphical curve relating the angular movement to the time, which was then compared to the desired position determined using the setpoint. The solution space of the system output has been obtained by utilizing the surface facility available in the adopted programming language. The best system output has been obtained through some different tuning actions.

C. Results of the Launcher Movement Experiments

The experiments have been done by tuning each output value of NB, NS, PS and PB, in order to get the system output and the solution space. The system responses to the control of azimuthal angle for various setpoint values are given in Figure 19 - Figure 22.

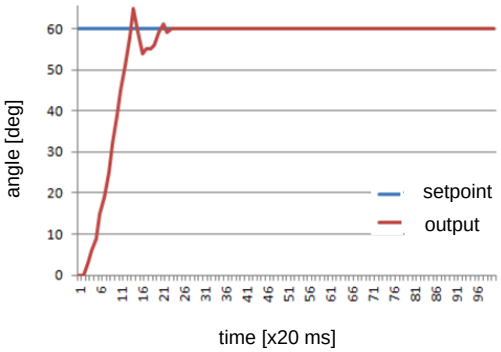

Figure 19: System Response for The Movement Control Along the Azimuthal Angle Using The Setpoint of 60^{O}

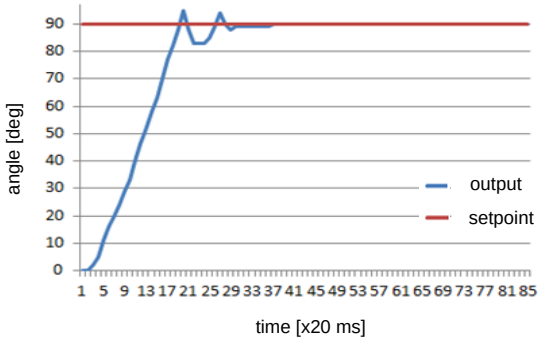

Figure 20: System Response for The Movement Control Along the Azimuthal Angle Using The Setpoint of 90^{O}

Figure 19 indicates the graphical output response of the output NB, NS, PS and PB using the setpoint of 60^{O} and the time sampling 20ms for the movement control along the azimuthal angle. It can be seen that the rise-time is around 0.28 second, and the settling point is situated on the 23rd sampling or after 0.46 second. Using the setpoint of 90^{O}, as seen in Figure 20, the rise-time is around 0.40 second, and the settling time is 0.74 second, which means that the settling point is started at the 37th sampling. It can be observed that higher the setpoint value, longer is the rise-time as well as the settling time.

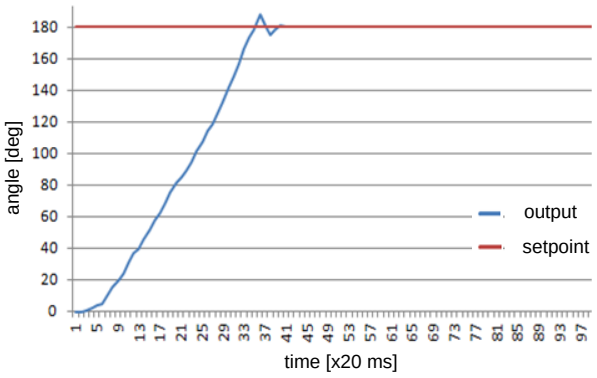

Figure 21: System Response For The Movement Control Along The Azimuthal Angle Using The Setpoint of 180^{O}

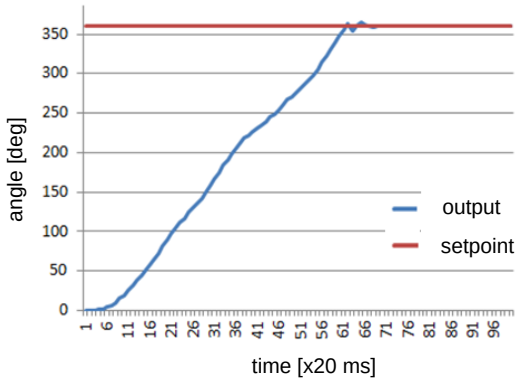

Figure 22: System Response For The Movement Control Along The Azimuthal Angle Using The Setpoint of 360^{O}

Using Figure 21 and Figure 22 we can compare the graphical output response of the output NB, NS, PS and PB using the setpoints of 180^{O} and 360^{O}. Using the time sampling of 20ms, it can be found that the obtained rise-time for the setpoint of 180^{O} and 360^{O} respectively are 0.72 second and 1.24second. The settling points have been reached after the 41st and 69th sampling, or respectively giving the settling time of 0.82second and 1.38second. It also confirms the previous statement that along the azimuthal angle control, higher the setpoint value, longer is the rise-time as well as the settling time.

The system responses to the control along the elevation angle for the setpoints of 15^{O}, 45^{O} and 60^{O} are given in Figure 23 - Figure 25 respectively.

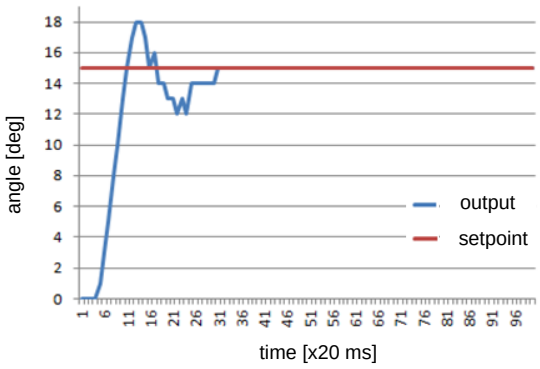

Figure 23: System Response for The Movement Control Along The Elevation Angle Using The Setpoint of 15^{O}

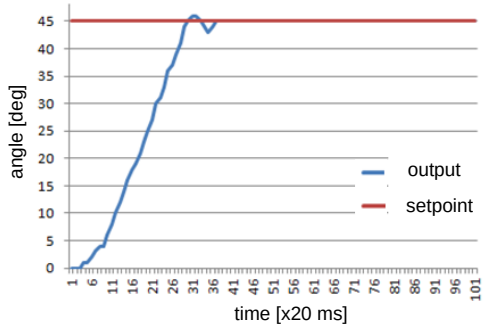

Figure 24: System Response for The Movement Control Along The Elevation Angle Using The Setpoint of 45^{O}

Figure 23 indicates the graphical output response of the output NB, NS, PS and PB with the setpoint 15^{O} and the time sampling of 20 ms for the movement control along the elevation angle. It can be seen that the rise-time is around 0.26 second, and the settling point is started at the 31^{st} sampling or after 0.62 second. Using the setpoint of 45^{O}, as seen in Figure 24, the rise-time is around 0.62 second, and the settling time is 0.74 second, which means that the settling point is started at the 37^{th} sampling. It can be observed that higher the setpoint value, longer is the rise-time as well as the settling time.

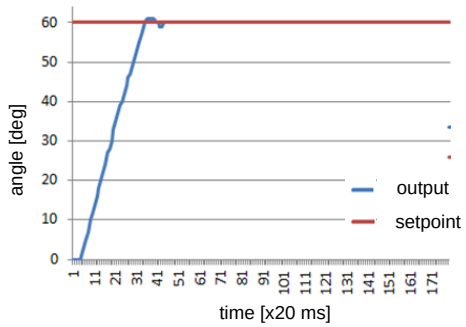

Figure 25: System Response for The Movement Control Along The Elevation Angle Using The Setpoint of 60^{O}

Figure 25 shows the graphical output response of the output NB, NS, PS and PB with the set-point of 60^{O}. Using the time sampling of 20ms, it can be found that the obtained rise-time for the set-point of 60^{O} is 0.72 second. The settling points have been reached after the 44^{th} sampling, or giving the settling time of 0.88 second. It confirms again the previous statement that along the elevation angle control, higher the set-point value, longer is the rise-time as well as the settling time.

The obtained results indicated by the previous graphical output responses for various set-point values, both during the azimuthal and elevation angles control, confirm that the output of the system is in accordance with the designed specifications. Both the testing of system components as well as the whole system showed the acceptable error percentages, which is less than 2%. The obtained steady-state error of 0% can be observed directly from the graphics at the time it starts to reach the settling points. The average rise time is 0.533 second during the control along the elevation direction, and 0.695 second along the azimuth direction.

IV. Conclusion

The analysis of the research results has brought into some conclusions that the *Rolex* rocket launcher board being embedded with an FL-PID mixed control technique could successfully direct the launcher movement into the desired position. The intelligent control was implanted into the Arduino Mega 2560. The values of error and delta error were becoming the inputs of the Fuzzy-Logic control. Their membership functions were to be determined to result in the desired values of K_p, K_i and K_d constants of the Proportional-Integral-Differential controller. The mixed control method has been proven well to process the input values. The action of directing the rocket launcher along both the azimuth and the elevation angles was executed by a driving motor based on the set-point given using a keypad. The range of elevation angle of rocket launcher's arm movement was from 0 to 70 degrees, while the movement along the azimuthal angle direction was from 0 to 360 degrees. The obtained average rise-time was 0.533 second during the elevation angle control and 0.695 second during the azimuthal angle control, giving a total average rise-time of 0.625 second with the steady-state error of 0%.

Acknowledgment

J. Saputra presents his sincere thanks to the Polytechnics of Indonesian Army (Poltekad), Indonesia for providing financial support enabling the publication and presentation of this research results, and to the Department of Electrical Engineering, Faculty of Engineering, Brawijaya University, Indonesia for the research collaboration the results of which are presented in this publication.

References

[1] Indrawanto, *The Development of Control System and Stabilization of Cannon Barrel Motion* (in Indonesian). Bandung: LPPM-ITB, 2007.

[2] M.A. Muslim, D. Minggu, J. Saputra, and R.N. Hasanah, "Comparison analysis between fuzzy and fuzzified-PID methods on gun-barrel motion control," *ARPN Journal of Engineering and Applied Sciences*, Vol. 10, No. 20, 9765-9771, November 2015.

[3] J. Saputra, R.N. Hasanah, and M.A. Muslim, "Target tracking of the S-60 single-barrel 57mm anti-aircraft gun system using hybrid control method," *ARPN Journal of Engineering and Applied Sciences*, Vol. 10, No. 19, 9071-9077, October 2015.

[4] B. Rosser, *Mathematical Theory of Rocket Flight*. New York McGraw-Hill Book Company, Inc., 2008.

[5] M.J.L. Turner, Rocket and Spacecraft Propulsion: Principles, Practice and New Developments. Chichester, UK: Praxis Publishing Ltd, 2009.

[6] G.P. Sutton and O.B. Biblarz, *Rocket Propulsion Elements*. New York: John Wiley & Sons Inc., 2000.

[7] R.N. Hasanah, S.I. Putri, and H. Suyono, "Optimization of sun-tracker positioning using Takagi-Sugeno fuzzy-logic method," *Applied Mechanics and Materials Periodical*, Volume 785, 231-235, 2015.

[8] K. Ogata, *Modern Control Engineering*. Singapore: Prentice Hall, 2010.

[9] I. D. Landau and G. Zito, *Digital Control Systems, Design, Identification and Implementation* . London: Springer-Verlag London Limited, 2005.

[10] H.M. Kim, K.T. Park, and S.J. Kim, "Adaptive back-stepping position control system with fuzzy neural networks algorithm," in *5th IEEE International Conference on Digital Ecosystems and Technologies (IEEE DEST 2011) Proceedings*, (IEEE Industrial Electronics Society, Daejeon, Korea, 2011), pp. 170-175.

[11] D. He and R. M. Nelms, "Fuzzy logic average current-mode control for DC-DC converters using an inexpensive 8-bit microcontroller," *IEEE Transactions on Industry Applications*, Volume: 41, Issue: 6, 1531–1538, Nov.-Dec. 2005.

[12] N. Gulley, Jang, J-S. Roger, *Fuzzy Logic Toolbox For Use with MATLAB*. The MathWorks, Inc., 2005.

[13] A. Verkeyn, D. Botteldooren, G. De Tre, and R. De Caluwe, "Fuzzy modeling of traffic noise annoyance," in *Joint 9th IFSA World Congress and 20th NAFIPS International Conference Proceedings*, edited by M.H. Smith, et al. (International Fuzzy Systems Association, North American Fuzzy Information Processing Society, in cooperation with IEEE Systems, Man and Cybernetics Society, IEEE Neural Networks Council, Piscataway, NJ, 2001).

[14] Z. Salleh, M. Sulaiman, and R. Omar, "Tuning fuzzy membership functions to improve performance of vector control induction motor drives," *Journal of Telecommunication, Electronic and Computer Engineering (JTEC)*, Vol 8, No 2, pp. 1-4, 2016.

[15] Y.S. Akil and Y. Mitani, "Seasonal short-term electricity demand forecasting under tropical condition using fuzzy approach model," *Journal of Telecommunication, Electronic and Computer Engineering (JTEC)*, Vol. 9 No. 1-3, pp. 77-82, 2017.

[16] G. Chen and T.T. Pham, *Introduction to Fuzzy Sets, Fuzzy Logic, and Fuzzy Control Systems*. New York: CRC Press LLC, 2001.

[17] C.C. Lee, "Fuzzy logic in control systems: fuzzy logic controller," *IEEE Transactions on Systems, Man, and Cybernetics*, Vol.: 20, Issue: 2, 404-435, Mar/Apr 1990.

[18] S.F. Barrett and D. Pack, *Microcontrollers Fundamentals for Engineers and Scientists*. New York: Morgan & Claypool Pulishers, 2006.

[19] S.F. Barrett, D. Pack, and Thornton, *Atmel AVR Microcontroller Primer: Programming and Interfacing*. New York: Morgan & Claypool Pulishers, 2008.

[20] N. Mohan, T. Undeland, and W.P. Robbins, *Power Electronics Converters, Applications and Design*. Canada: John Wiley & Sons, Inc., 1983.